# Nanowire and nanotube transistors for lab-on-a-chip applications

**Minbaek Lee,[a] Ku Youn Baik,[a] Meg Noah,[b] Young-Kyun Kwon,*[bc] Jeong-O Lee*[d] and Seunghun Hong*[a]**

***Received 13th March 2009, Accepted 21st May 2009***
***First published as an Advance Article on the web 16th June 2009***
**DOI: 10.1039/b905185f**

Implementation of one-dimensional nanostructure-based devices in the lab-on-a-chip framework can allow us to impart various functionalities such as highly-sensitive sensors to a single chip. However, it is still extremely difficult to position nanowires or nanotubes on a defined area of solid substrates to build integrated functional devices. Herein, we review promising strategies for the massive integration of nanowires/nanotubes on lab-on-a-chip and their practical applications to sensors. The theoretical understanding and sensor characteristics of nanowire/nanotube-based devices are also discussed.

## 1.0 Introduction

Recent advances in nanotechnology have enabled chemical or biological detection with high spatial resolution as well as the manipulation of individual molecules. For sensor applications, the size of the sensors compared to that of target molecules is one of the most important factors determining their detection limit. For this reason, an ideal building block for sensor fabrication can be one-dimensional (1D) nanostructures such as nanowires (NWs) and carbon nanotubes (CNTs) which already have shown their high sensitivity to chemicals and biomolecules. Combining these new components to lab-on-a-chip (LoC) formats brightens the prospect of developing advanced tools for the investigation of biochemistry and life processes. However, their ultra-miniatured size produces not only extraordinary performance but also the difficulties in handling and positioning the NW/CNT-based devices on the desired locations of LoCs. As a matter of fact, a difficulty in the massive positioning of NW/CNT-based devices has significantly delayed their practical applications for LoCs.

In this review, we will discuss several important issues regarding NW/CNT-based transistors for LoC applications: (1) the massive integration methods of NW/CNT-based transistors for LoC applications, (2) biosensors based on semiconducting NWs or CNTs, and the possibilities of integrating them with LoC systems, (3) the theoretical understanding of CNT/NW-based transistors and sensors.

## 2.0 Massive integration of nanowire/nanotube transistors to lab-on-a-chip applications

One of major technological bottlenecks for 1D nanostructure-based devices for LoC application is a lack of fabrication methods into massive parallelism. Although tremendous efforts have been made to solve this problem, NW/CNT-based devices have not been extensively utilized for LoC applications. Presumably, it is because the practical mass fabrication method of these superb materials has not been established yet. In this section, we will overview several promising mass fabrication methods of NW/CNT-based devices such as selective and controlled growth, directed-assembly and printing technologies of NWs/CNTs for LoC applications.

[a]*Department of Physics and Astronomy, Seoul National University, Kwanak-Gu, Shillim-Dong, Seoul, Korea. E-mail: shong@phya.snu.ac.kr; Fax: +82 2-884-3002; Tel: +82 2-880-1343*
[b]*Department of Physics and Applied Physics, University of Massachusetts, Lowell, MA, 01854, USA*
[c]*Department of Physics and Research Institute for Basic Sciences, Kyung Hee University, Hoegi-dong, Dongdeamun-gu, Seoul, 130-701, Korea. E-mail: ykkwon@khu.ac.kr; Fax: +82 2-957-8408; Tel: +82 2-961-9279*
[d]*NanoBio Fusion Research Center, Korea Research Institute of Chemical Technology, Shinseong-no19, Eusung-gu, Daejeon, 305-343, Korea. E-mail: jolee@krict.re.kr; Fax: +82 42-860-7508; Tel: +82 42-860-7336*

*Minbaek Lee received his B.S. degree in Physics Education from Seoul National University in 2003. He is currently a PhD candidate in the Physics department at Seoul National University under the supervision of Prof. Seunghun Hong. His current research topic is the directed-assembly of carbon nanotubes/nanowires on solid substrates for various device applications.*

*Ku Youn Baik received her PhD degree in Biophysics from the Seoul National University under the supervision of Kwang-Sup Soh in the fall of 2008. Her research focus was measuring elasticity of microparticles from tissues using an atomic force microscope. Her current research focuses on application of CNT networks to the modulation and the detection of stem cell physiology.*

### 2.1 Selective growth strategy

A well-known self-organized growth method for creating NWs and CNTs is the chemical vapor deposition (CVD) process, while CNTs were first produced using an arc-discharge evaporation method by Iijima.[1] The earliest and principal growth concepts always employed the metal catalysts or the epitaxial thin films as seed particles. In this prevailing 1D nanostructure growth method, it is apparent that the selective positioning of NW arrays can be achieved by the preparation of well-ordered catalyst arrays. For decades, various catalyst patterning techniques have been proposed to provide controlled arrangements of catalysts, such as micro-contact printing (MCP),[2] photolithography,[3] atomic force microscope (AFM) lithography,[4] electron-beam lithography (EBL),[5,6] nanosphere lithography,[7] nanoimprint lithography (NIL),[7] and other self-assembled templates including block copolymers and anodic aluminium oxides (AAO).[8]

Such representative examples are shown in Fig. 1. Fig. 1 (a) shows the single-walled carbon nanotube (SWNT) channel array grown on a predesigned catalyst patterns by the MCP method.[9] In this case, a liquid phase catalyst precursor film was transferred onto the top of the poly-Si substrate by contact printing using a polydimethylsiloxane (PDMS) elastomeric stamp, and then electric fields have been exploited to align CNTs into desired direction during the growth process.[2]

One growth framework compatible with current Si industry is the method using photolithography for patterning catalysts. Fig. 1 (b) shows the SEM image of the perfectly aligned array of CNTs grown from the lithographically-patterned catalysts on quartz substrates.[3] This technique has been utilized to demonstrate the use of dense and aligned CNT arrays as an effective thin-film semiconducting materials suitable for integration of transistors and other electronic devices.

EBL and metal lift-off methods also can be utilized to pattern the periodic array of catalysts on substrates.[5,6] In Fig. 1(c), InP NW arrays were grown from the patterned gold particles using the metal–organic vapor phase epitaxy (MOVPE) method. The lithographic patterning strategy of the catalysts allows massive control over individual NWs.

Fig. 1 (d) shows the use of NIL to define the array of catalysts. Subsequently, the growth of vertically aligned InP NWs was accomplished by the MOVPE technique. Compared to EBL

*Meg Noah received her B.S. degree in physics from University of Toledo, and M.S. degree in Applied Physics from Johns Hopkins University Whiting School of Engineering. She is currently a PhD candidate in the physics department at University of Massachusetts at Lowell under Dr Dan Wasserman. Her current research topics focus on the design, characterization, and modeling of novel materials and devices.*

*Jeong-O Lee got her PhD degree from Chonbuk National University, and then moved to TUDelft for her postdoc. After working on molecular devices and nanotube sensors for two years under the guidance of Professor Cees Dekker, she moved into Korea Research Institute of Chemical Technology at 2003. Since then, she is working on nanoscale devices and sensor applications of them, details regarding her research can be found at http://nbalink.krict.re.kr.*

*Young-Kyun Kwon received his B.S. (1990) and M.S. (1992) from Seoul National University, and his PhD in Physics (1999) from Michigan State University. He worked as a postdoctoral fellow at UC Berkeley (2000, 2004–2005), as a senior scientist at Nanomix, Inc. (2000–2004), and as an assistant professor of physics at the University of Massachusetts at Lowell (2005–2008). Since 2008, he has been an associate professor of physics at Kyung Hee University, Seoul, Korea. His research interests include computational studies on nanostructured materials, surfaces and interfaces, and modeling of potential applications such as hydrogen storage, nanoelectronics, sensors, and OLED.*

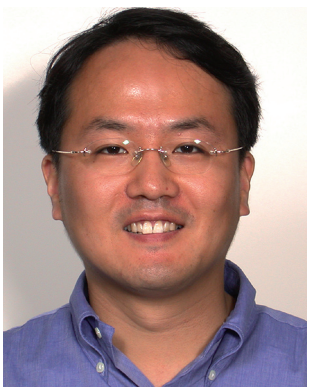

*Seunghun Hong finished his PhD in Physics (1998) at Purdue University. He worked as a postdoc and research professor in Chemistry Department at Northwestern University from 1998 to 2001. He was an assistant professor in the Physics Department at Florida State University from 2001 to 2003. Since then, he has worked as an assistant (2003–2005) and associate (2006-now) professor in Physics Department at Seoul National University. His research fields include molecular electronics, dip-pen nanolithography, self-assembly, surface-programmed assembly, CNT electronics, nano-biosensors, nanoscale tissue engineering, and biological motors.*

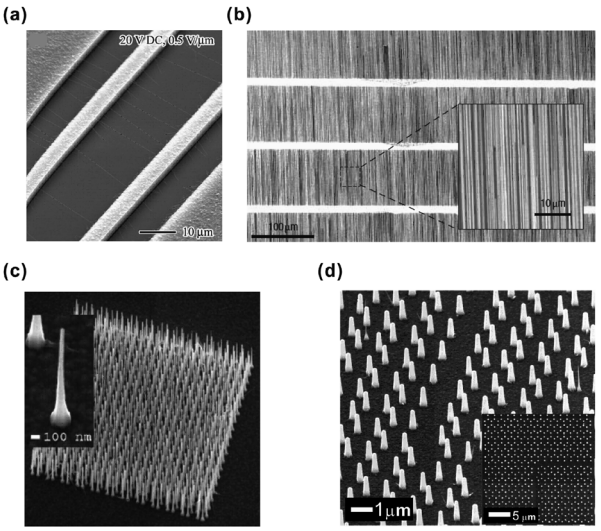


**Fig. 1** (a) SEM image of suspended SWNTs grown from MCP patterned catalyst under an electric field. The spacing between the outer poly-Si electrodes is 40 μm. (b) SEM image of a pattern of aligned SWNTs formed by CVD growth on a quartz substrate. The bright horizontal stripes correspond to the regions of iron catalyst patterned by photolithography. The inset provides a magnified view. (c) SEM image of a high-density array of InP (111) NWs on Au catalyst patterned substrate by e-beam lithography. (d) Tilted SEM image of NIL-defined InP nanowire arrays as obtained after growth. Inset shows a top view, displaying the high perfection and uniformity of the arrays. Image (a) adapted from Ref. 2, (b) from Ref. 3, (c) from Ref. 5, and (d) from Ref. 7.

method, NIL method has many advantages such as producing patterns at a considerably lower cost and with a higher throughput.

### 2.2 Directed-assembly strategy

Even though selective growth method allows one to position high-purity NWs or CNTs on desired locations, it is somewhat problematic to mass-produce NWs on a large-scale with desired locations. Furthermore, some of NWs can be only mass-produced by the solution-phase synthesis. Compared to the vapor-phase growth method, solution-phase synthesis has various advantages such as inexpensive instruments, rather low temperatures, and convenience in compound alteration. These advantages allow it to be very promising for the large-scale synthesis of NWs. Solution-based chemical synthesis has different synthetic frameworks based on controlled precipitation from homogeneous solutions such as hydrothermal/solvothermal process,[10] solution–liquid–solid (SLS) process,[11,12] solution-phase method based on capping reagents,[13–15] and low-temperature aqueous-solution process.[16,17] Somehow, to build these 1D nanostructures into practical applications on LoCs, the NWs in a solution must be assembled onto the specific locations on the substrate with accurate direction. This section will focus on the directed-assembly strategy of pre-grown NWs and CNTs.

**a. Assembly methods based on external guiding forces.** With the support from guiding forces, various directed-assembly techniques have been developed to build massive NW array on the chip using pre-grown 1D nanostructure solutions. One example is the dielectrophoresis method which utilizes electric field to position NWs due to their highly anisotropic structures and large polarization (Fig. 2 (a)). Smith and colleagues demonstrated the e-field assisted assembly of metallic NWs,[18] and Krupke *et al.* applied it for separation and assembly of CNTs (Fig. 2(a) left).[19] Here, the polarization of the NWs in alternating electric field resulted in attracting or repelling forces depending on applied voltages and AC frequency. Recent work also shows the assembly of individual NWs into parallel and crossed arrays,[20] which proved the dielectrophoresis method suitable for organizing individual NWs with good directional and spatial controls. Lately, Mayer *et al.* demonstrated DNA-coated hybrid

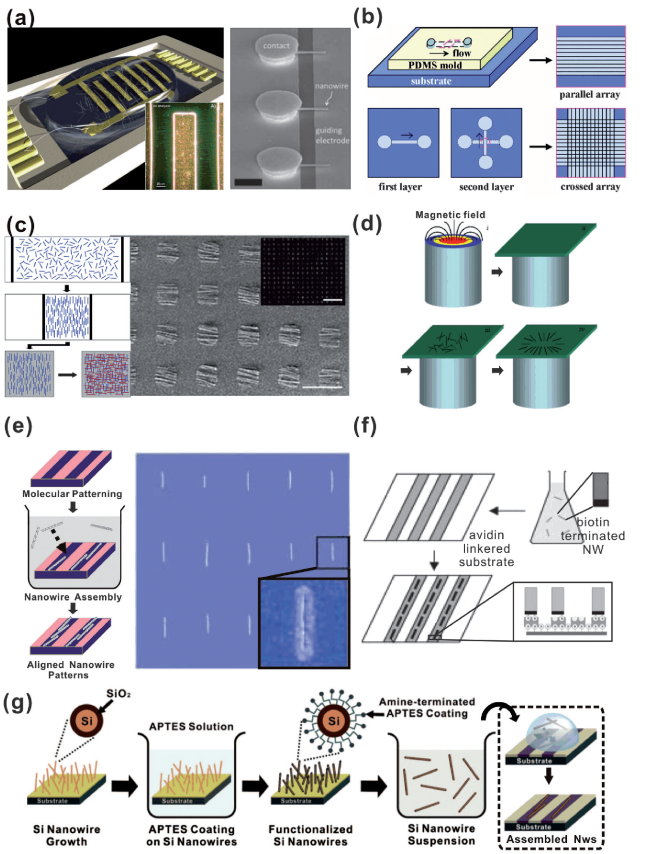


**Fig. 2** (a) Illustration of the dielectrophoresis experimental setup, showing microelectrodes wired to an ac field (left). Inset shows Rayleigh scattered light from the dielectrophoretically deposited CNTs. SEM image of DNA-coated hybrid device array driven by dielectrophoresis (right). (b) Schematic diagram of fluidic channel structures for flow assembly. (c) Schematic diagram of Langmuir–Blodgett technique (left). SEM image of hierarchically patterned 10 μm × 10 μm parallel NW arrays (right). Scale bar is 25 μm. Inset shows large area dark-field optical micrograph of patterned parallel NW arrays. The inset scale bar is 100 μm. (d) Schematic of magnetic field assembly. (e) Schematic diagram of surface-programmed assembly (left). Topography (30 μm × 30 μm) of an array of individual SWNTs (right). Inset shows AFM image of a single SWNT. (f) Schematic diagram of bio-recognition directed assembly. (g) Schematic diagram of the preparation method of amine-functionalized Si NW suspensions and assembly method. Image (a) adapted from Ref. 19 and 21, (b) from Ref. 22, (c) from Ref. 25, and (d) from Ref. 27, (e) adapted from Ref. 29, (f) from Ref. 35, (g) from Ref. 38.

NW device arrays using the dielectrophoresis strategy (Fig. 2(a) right).[21]

A physical fluidic-flow can be utilized to align NWs and CNTs as a guiding force (Fig. 2(b)).[22] In brief, they assembled arrays of NWs by passing suspensions of the NWs through fluidic channel structures formed between a PDMS structure and a flat substrate (Fig. 2b). Parallel and crossed arrays of NWs have been also fabricated using crossed flows.

One method for the assembly of anisotropic building blocks is the Langmuir–Blodgett (L–B) technique (Fig. 2(c)).[23–25] In this method, the NW suspension was spread on the water surface. The NW surface layer was then compressed slowly to closely pack in confined surface area. At proper stages of compression, the aligned NW packs at the water–air interface were transferred carefully onto desired substrates or donor substrates for the next building steps such as a layer-by-layer process.[25]

The other method is a magnetic force-driven self-assembly process.[26,27] It employs a magnetic field to align and position magnetic NWs such as nickel, cobalt, and permalloy (Fig. 2(d)).[27] Tanase *et al.* demonstrated that magnetic NWs in liquid suspension can be manipulated and assembled on substrates using a combination of external and locally applied magnetic fields.[26] In this work, Ni NWs were assembled and aligned on top of predefined ferromagnetic electrodes under the high magnetic field. In recent works, cross junction and T-shape junction of NW networks were also demonstrated using sequential magnetic field operations.[27]

**b. Assembly methods based on internal interactions.** Concurrently with assembly techniques guided by external forces, internal molecular forces have been also utilized in directed-assembly process. In case of SWNT assembly, chemically modified substrates were utilized to induce internal interaction of selective assembly, and it was recently named as a "surface-programmed assembly" (SPA) method.[28–32] In this process, self-assembled monolayer (SAM) patterns were prepared on solid substrate *via* various methods such as MCP,[9] DPN[33,34] and also photolithography.[30,31] The SAM patterns were used to direct the adsorption and alignment of NWs on solid substrates in the suspensions. Using this strategy, various nanostructures including $V_2O_5$ NWs,[30] CNTs,[29,30,32] and Si NWs[38] were successfully assembled on solid substrates with high precision (Fig. 2(e)). In this work, the substrates were first functionalized with SAM molecules to create surface charge or polarization, while covering counter-region as non-polar molecules. For CNT assembly on $SiO_2$ substrate,[30] bare $SiO_2$ and octadecyltrichlorosilane (OTS) were utilized as polar and non-polar SAM regions, respectively. When the substrate was placed in the solution of CNTs, the CNTs were attracted to polar regions due to van der Waals-type interactions. It can be also applied to the assembly of other NWs with different charges. Since the adsorbed NWs/CNTs form stable structures, one can continue additional microfabrication steps to fabricate functional devices such as field effect transistors (FETs) on a chip.

Bio-recognition directed assembly is also an attractive method to position nanostructures into functional devices because of their highly specific nature offered by biomolecules such as proteins[35,36] and deoxyribonucleic acid (DNA).[37] Salem *et al.* applied the receptor-mediated assembly method to assemble a large number of multicomponent NWs (Fig. 2 (f)).[35] They anchored two segment Au/Ni NWs to desired location on the substrate using the biotin–avidin linkage, which is one of the well-known biological interactions with stability over a wide pH range. More importantly, these biological linking systems can be also a means for biological applications in LoC.

Some NWs such as Si NWs are quite difficult to disperse into solution with controlled surface functionalities due to their inherent properties or contaminations during multiple processing steps. Recently, Heo *et al.* reported a simple but efficient method for dispersing Si NWs in solution and also assembling them into virtually general shape patterns (Fig. 2 (g)).[38] In this method, Si NWs grown by CVD method were modified with 3-aminopropyltriethoxysilane (APTES) SAM to prepare well dispersed aqueous solution of Si NWs. Then, the SPA method has been utilized for the selective assembly of functionalized Si NWs (Fig. 2 (e)). In this case, Si NWs were adsorbed onto negatively-charged surface regions such as bare $SiO_2$ surfaces or SAM patterns terminated with carboxyl groups. The APTES coating as well as native oxide layer on the assembled Si NWs could be removed by a wet etching process to achieve intimate contacts with the electrodes or alter the chemical functionalities.

### 2.3 Printing strategy

Although the selective growth and assembly strategies have clearly shown the possibility for the practical applications, the assembly of NWs and CNTs on soft substrates including plastic substrate requires a new paradigm and excluded any processes including high temperature or reactive chemical treatment steps. Here, we will review the recent developments of the printing technologies to deliver NWs and CNTs to specific locations of soft substrates.

One of the most powerful tools for moving NWs to soft materials is the dry transfer printing method which was first developed by Roger's group. This method has been extensively utilized for transporting nanostructures[39–41] and CNT networks[42] on flexible substrate (Fig. 3 (a)). In this method, elastomeric stamps are utilized to peel off the patterned nanostructures from the donor substrate and then to transfer them onto the receiving substrate. Various techniques have been utilizled to improve the efficiency of the transfer process. One successful strategy is relying on viscoelastic properties of elastomeric stamps. In this case, predesigned nanostructures are first fabricated on solid substrates using top-down approach, bottom-up growth, self-assembly or other techniques. Then, an elastomeric stamp makes a first contact with the donor substrate. Pulling the stamp away from the donor substrate with sufficiently high peel velocity leads to adhesion that is strong enough to keep the desired objects attached on the surface of the stamp. Removing the stamp with sufficiently low speed causes the objects to adhere preferentially to the receiving substrate rather than to the stamp. The strength of adhesion between the stamp and the nanostructure depends on the peel speed due to the viscoelastic properties of the stamp.[41]

More facile printing method might be using the MCP process itself to directly deposit nanostructures.[9] Fig. 3 (b) showed schematic diagram depicting $V_2O_5$ NW patterning using the MCP technique.[43] In the work, the solution of $V_2O_5$ NWs were deposited on a PDMS stamp and solvents were blown with $N_2$

 

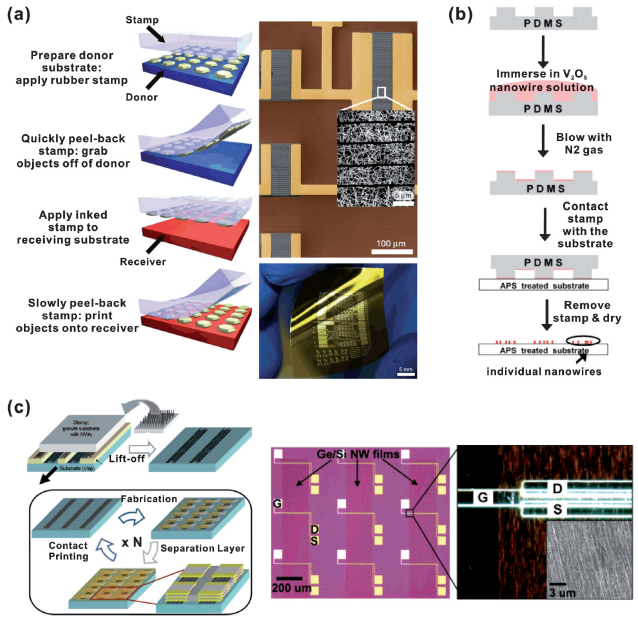


**Fig. 3** (a) Schematic diagram of Dry-transfer printing method (left). Scanning electron microscope image as part of the transferred SWNT network circuit (right upper). Photograph of a collection of transferred SWNT transistors and circuits on a thin sheet of plastic (right bottom). (b) Schematic diagram of microcontact printing. (c) Schematic diagram of direct contact printing (left). Optical microscope image shows the array of three-dimensional NW FETs. Inset shows SEM image of Ge/Si NW array. Image (a) adapted from Ref. 41 and 42, (b) from Ref. 43, (c) from Ref. 45.

gas. The inked stamp with NWs was directly contacted with the desired substrate and transferred NWs onto it.

The other facile direct printing method was demonstrated by Lieber's group. They achieved wafer-scale assembly of highly ordered, dense NWs with high uniformity through a simple contact printing process (Fig. 3 (c)).[44] This contact printing method involves directional sliding of a donor substrate, consisting of densely-grown NWs, on a receiving substrate covered with a desired resist pattern. During the process, NWs are effectively adhered to receiving substrate by the van der Waals interactions between NWs and the receiving substrate. Using this technique, they also demonstrated three-dimensional multifunctional electronics based on the layer-by-layer assembly of NWs.[45]

## 3.0 Sensors based on nanowire/nanotube devices

Apart from practical applications, the largest contribution nanotechnology has made may be the opening of multidisciplinary science. Electronic devices, which were not remotely related with biotechnology before, now combined with biomolecules to provide state of the art diagnostic sensors that can monitor even a few-disease-related biomolecules.[46] Such a union started to carry weight only when the size of the electronic device component comparable to that of biomolecules, since the sensitivity can be greatly improved. For example, the diameter of semiconductor NW is ~10 nm, and that of SWNT is ~1 nm, while antibodies or enzymes are around 10 nm big. Apart from ultimate sensitivity, massively parallel multiplexing is an another virtue that nanobiosensors should carry, since multiplexing enables the diagnosis of multiple diseases at the same time or that of the complex diseases such as heart diseases or cancer. In that end, nanoelectronic devices such as semiconductor NW or SWNT FET can be an ideal candidate for future diagnostic sensors. Sensitivity can be achieved *via* high mobility nanoelectronic devices, and massive arrays of nanodevices can be possible through recent advancement of top-down and bottom-up fabrication techniques. In this review, we introduce biosensors based on semiconductor NWs and SWNTs, and discuss the possibilities of integrating them for LoC applications.

### 3.1 Nanowire FET biosensors

Emergence of nanoFET sensors was only started at 21st century, after the pioneering work of Cui *et al.*[47] in NW sensors, and Kong *et al.* in nanotube sensors.[48] In Cui *et al.*'s work, boron-doped *p*-type Si NW device grown by vapor-liquid-solid (VLS) method was covalently modified with 3-amino-propyltriethoxysilane (APTES), that can undergo protonation and deprotonation according to the pH in the medium. Sensing mechanism was suggested as "chemically gated transistor" bound target molecules can deplete or accumulate charge carriers in nanostructures. To supply target molecules, a microfluidic channel made of polydimethylsiloxane (PDMS) was attached on top of the device as well. After this, numerous biosensors that use semiconductor NW FETs or SWNTs were demonstrated. Most of the NW FET sensors are made of Si, though there are sensors fabricated with $In_2O_3$[49] or ZnO NWs as well.[50] Preference of Si NW over other materials can be understood in two respects. First, due to the high mobility of silicon, it is possible to achieve highly sensitive sensors, and second, surface chemistry is well known, as well as doping control in silicon based electronics.

Most of the nanoFET sensors reported are immunosensors based on antibody–antigen binding. As shown below, Patolsky *et al.* modified multiple NW devices with virus-specific antibodies to yield selective detection of virus particles.[51]

Authors combined the confocal microscope image with the electrical measurement to relate the binding of virus particles with sensor signals. Conductance decreases abruptly when virions bind with antibody-modified Si nanoFETs, and restores to its baseline after unbinding, thereby showed the possibility of highly sensitive (100 virions/μl) virus sensor (Fig. 4).

Assessment of multiple tumor markers has been achieved by Zheng *et al.*,[52] using Si NW devices modified with monoclonal antibodies (mAb) specific to prostate specific antigen (PSA), carcinoembryonic antigen (CEA) and mucin-1. Through multiplexing, one may expect to get more information necessary for diagnose complex diseases like cancer, and due to the high sensitivity (~fM detection limit), diagnosis can be made at the very early stage of disease. Also, authors showed that surface charges of target molecules are indeed responsible for observed change of conductance upon target binding, by employing *p*-type and *n*-type nanoFET at the same time. With the same target, while *p*-nanoFET showed increase of conductance, n-nanoFET showed decrease of conductance due to the electron depletion by target binding. False signals coming from non-specific binding can be eliminated by this method as well.

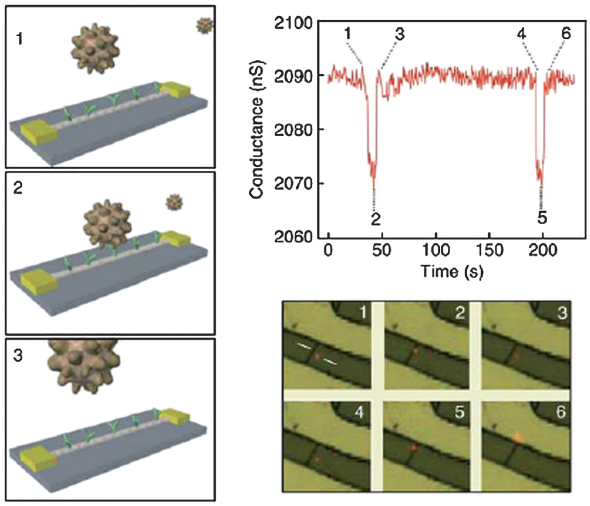


**Fig. 4** Schematic diagram of the nanotube virus sensor (left), real-time electrical measurement from device (top right), and confocal laser microscope image of the device with dye-labelled virions (bottom right). Images adapted from Ref. 51.

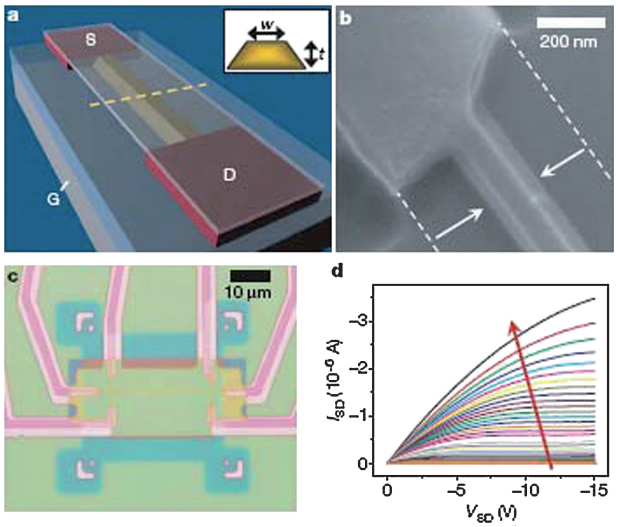


**Fig. 5** Si nanowire device fabricated by top-down approach. (a) Schematic diagram of the device. (b) SEM image of such device. (c) Optical micrograph. (d) Electrical characteristics of the device. Red arrow points in the direction of the applied negative gate voltages (*p*-type FET). Images adapted from Ref. 53.

Until recently, Si nanoFETs fabricated *via* bottom-up approach showed superior sensing performance compared with nanoFETs fabricated with top-down method. Synthesized NWs are single crystalline without any defect, and thanks to the recent advances in self-assembly (in chapter 1), massive bottom-up arrays based on synthesized NWs are possible. On the other hand, top-down fabricated nanoFETs can offer uniformity of devices, and large scale production is possible through already established CMOS fabrication process.

The disadvantage of top-down NW FET, having defects due to the dry etching process, was resolved by Stern *et al.*[53] Stern *et al.* succeeded to fabricate silicon NWs without mobility degradation by top-down approach, using ultra-thin silicon on insulator (SOI) wafers (Fig. 5). High performance Si NWs thinner than the lithographically defined pattern could be obtained through the anisotropic etching of Si using tetramethylammonium hydroxide (TMAH). Fabrication of defect-free Si nanostructures using SOI wafers and TMAH was introduced by Menard *et al.* some years earlier.[54] Si nanostructures produced by this method can be transferred to another (flexible) substrates by contact printing or solution casting, and thin film transistors fabricated with Si nanostructures show mobilities as high as 180 $cm^2$/Vs on plastic substrates.

In the work of Stern *et al.*, bare NW FETs show logarithmic dependence of conductance with pH variation due to the protonation and deprotonation of surface oxide, and the greater sensitivity could be achieved with smaller diameter NW devices. To demonstrate the monitoring of specific binding of target with receptors, authors immobilized receptor molecules by using dec-9-enyl-carbamic acid tert-butyl ester, since this molecule has been shown to confer amine functionality directly to silicon. Since it has been shown that sensitivity decreases as surface modification layer for receptor immobilization increases,[52] it could be a good alternative to immobilize receptors directly on silicon surface instead of oxide surface. Highly sensitive biomolecule detection was demonstrated using a biotin–streptavidin pair, as well as antibody-triggered immune response from T cells. Sensors show sub-100 fM specific, label-free detection, and this approach is also meaningful in a sense that one can get highly sensitive sensors that can be integrated with CMOS technology.

Apart from immunosensors, varieties of biological contents could be screened using NW FET sensors. DNA sensors based on peptide nucleic acid (PNA) immobilized NW devices were demonstrated,[55] and interaction between small-molecules and protein could be monitored by using Si NW sensors as well.[56] Miniaturized device arrays that can directly monitor small-molecule–protein interaction could be valuable for pharmaceutical industry, since the interaction between small molecules and proteins or cell can lead to new drug discovery and screening.

### 3.2 Nanotube FET biosensors

In 1998, Tans *et al.* showed that a SWNT can be built as a single molecule transistor.[57] Since then, research efforts were focused on developing high performance nanotube devices including transistors, diode, logic gates and sensors. Mobility of SWNTs are much higher than that of silicon, and ballistic transport in SWNTs make them even more attractive for sensor applications.[58] Indeed, SWNT devices show extreme sensitivity toward $NO_2$ and $NH_3$ gases,[48] and the first generation nanotube sensors are already on the market.[59] Nanotube sensors reported to date can be divided into two categories. In the first category, devices contain only one or small number of semiconducting nanotubes, and show high mobility as well as on/off ratio. Devices belong to the second category consists of networks of nanotubes. Such classification is inevitable since we do not have synthetic methods to grow nanotubes with uniform chirality. Electronic properties of SWNTs depend on chiral angle how graphene sheets rolled into a cylinder, and there is no concrete method to control chirality developed yet. Therefore, yield of the devices in the first category is rather low, or one needs chemical[60] or electrical

sorting[61] to ensure single semiconducting behavior. On the other hand, mass production of network SWNT devices are possible, at the cost of mobility. Recently, large scale separation methods such as sedimentation[62] and chemical treatment[63] are being developed, for network devices with better quality.

As in the case of NW sensors, immunosensors based on SWNT-FETs were successfully demonstrated. For sensor operation, receptor antibodies can be coupled on the sidewalls of SWNTs *via* simple non-specific adsorption, non-covalent binding or covalent immobilization. Receptors with histidine or tryptophan residues were shown to have specific affinity toward SWNTs by phage display technique,[64] therefore could be directly incorporated on the nanotube surface without the aid of linking molecules. In most cases, however, covalent linkers that bind with the carboxyl groups in acid-treated SWNTs[65] or non-covalent linkers that can adsorb on SWNTs and bind with biomolecules *via* covalent binding were used for biosensors. Non-covalent binding linkers may preserve electronic properties of SWNTs, and non-covalent binding linkers were successfully used for detection of biotin–streptavidin binding,[66] autoimmune diseases,[67] and cancer marker detection.[68] There have been debates regarding the sensing mechanism of SWNT-FETs, since SWNTs function as a Schottky transistor (Fig. 6).[69] At the current stage, both Schottky barrier modulation and field effects are believed to play a role in nanotube sensors.[70] In that prospects, SWNT-FETs that utilize their contact electrodes as effective sensing surface have been shown as well. Tang *et al.*[71] and Gui *et al.*[72] showed label-free DNA sensors based on SWNT-metal barrier modulation. On the other hand, Byon and Choi decorated the SWNT surfaces with metallic nanoparticles to increase the Schottky junction area, and thereby improve the sensitivity.[73] They report a $10^4$ times increase in sensitivity (10 nM to 1 pM).

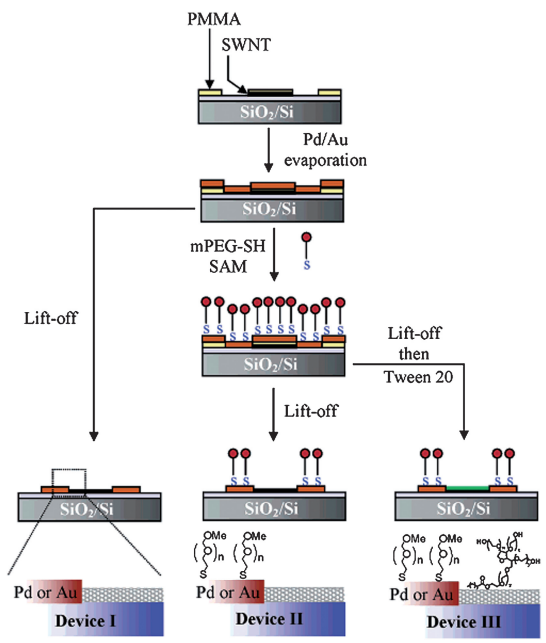


**Fig. 6** Schematic diagram of the experiments that show effective sensing areas in nanotube sensors. Images adapted from Ref. 69.

Still, the role of contact-Schottky barrier in nanotube network devices requires more systematic study, since contact barrier effect in nanotube network devices is expected to be smaller than that of single nanotube device due to the presence of multiple tube junctions.

### 3.3 Progresses and limitations of nanoFET biosensors

In this chapter, we introduced biosensors based on nanotube or NW FETs. Although extreme sensitivity and multiplexing may be achievable with those sensors, there are other problems that need to be overcome. In principle, nanoFET sensors are label-free since they recognize the change of electric field induced by biomolecules binding. However, such recognition is not feasible in physiological conditions due to the screening effect from surrounding ions.[74] Most of the nanoFET sensors reported function in low-ionic environment, and body fluids normally used for diagnostics (blood, urine, saliva, sweats) contains large amount of salts. To circumvent this problem, researchers suggested to use a smaller recognition element so that binding event can happen nearer to the sensor surface, where screening by surrounding ions is less effective. So *et al.* employed aptamers as molecular recognition elements,[75] and Maehashi *et al.* showed that indeed one can get more freedom with aptamers.[76] Also, fragment antibodies play a similar role in nanoFET sensors (Fig. 7).[77]

Another obstacle in nanoFET sensors can be the tiny sensing area. As pointed out by Squires *et al.*,[78] most nanosensors concentrate on binding kinetics of target molecules, but care only little about how target transported to the sensor surface. Considering that a solution with femtomolar target concentration has only one molecule in 1 nanolitre volume (100 μm × 100 μm × 100 μm),[78] it is difficult to expect target molecules to arrive at the sensor surface by simple diffusion. If we model NW sensor as a strip that is 10 nm wide and 2 μm long, and placed in a microchannel with 100 μm wide and 100 μm tall, one molecule in every 210 min can bind with NW sensor (for a microsensor 50 μm wide and 100 μm long, one molecule in every 6∼7 s will bind) in 10 fM target solution (Fig. 8). Certainly, this simple model cannot explain the actual situation, but would be useful for designing sensors. One way to break such a "speed limit" could be parallel NW sensors. Recently, So *et al.* demonstrated sensing of Escherichia coli (*E. coli*) using arrays of aptamer-immobilized SWNT-FETs. Instead of a single SWNT-FET, arrays of SWNT-FETs combined with statistical methods were used for the detection of *E. coli* to improve sensitivity.[79]

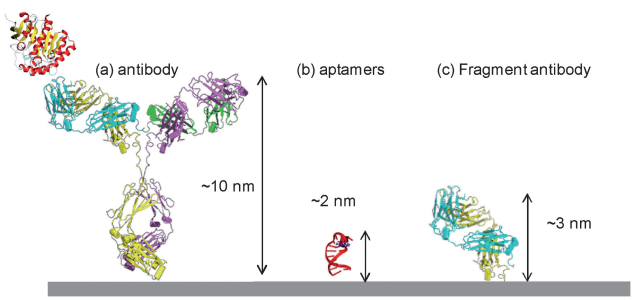


**Fig. 7** Size comparison between molecular recognition elements.

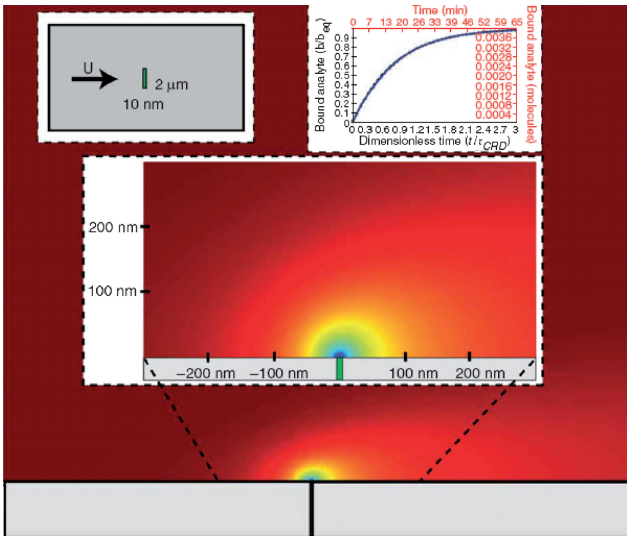


**Fig. 8** Steady-state depletion zone in nanowire sensors. Images adapted from Ref. 78.

Or, as suggested by the authors, electrostatics,[80] removing depletion layers by mixing,[81] or supply concentrated target solutions to the sensor surface[82,83] can be used to accelerate binding. In that sense, fusing microfluidic channels with specific functions is not just desirable, but becoming a necessity for practical applications of nanoFET sensors.

## 4.0 Device and sensor characteristics of nanowire/nanotube transistors

Since the invention of the integrated circuit, the number of transistors on a given area of an integrated circuit has doubled every 18 to 24 months for the last half century as Moore's law indicated.[84] It would be, however, within a few years that such a trend will stop in current top-down Si-based technology due to serious obstacles.

Some of the most important issues in the further reduction of the dimensions of transistors through the current top-down approach are whether their electronic characteristics remain unchanged and whether their geometries and functionalities are stable or reliable within their required lifetime. Such issues include increased off-current, increased current density, hot electrons, leakage current, carrier velocity saturation, and so on.[85]

After the discovery of CNTs in 1991,[1] it has been shown that they can be used as electronic devices such as field effect transistors.[57,58,86,87] Other semiconducting NWs including Si NWs have also been discovered or synthesized and investigated for their transistor behaviours.[88–92] Use of NWs including CNTs to build new electronic devices is being regarded as a potential breakthrough to overcome the scaling issues. These successful demonstrations raised an expectation that these NTs and NWs would be fundamental building blocks of future nanoelectronics replacing current bulk Si- or MOSFET-based traditional electronics, and thus the trend of Moore's law would continue for another decade or two at least.

In this section, we will briefly describe the theoretical understanding of the device and sensor characteristics of NT/NW based transistors, especially focusing on network-based transistors.

### 4.1 Basic theoretical understanding of nanowire/nanotube transistors

The minimum conductance of metallic CNTs is expected to be 2 $G_0$, where $G_0 = 2e^2/h \approx (12.9\ \mathrm{k\Omega})^{-1}$ is the quantum conductance,[93–95] according to the scattering theory.[96] While the delocalization of the wave function along the tube axis was observed experimentally more than a decade ago,[86,97] the conductance quantization for SWNTs was recently revealed.[98] It is believed that electrons propagate without inelastic scattering in perfect single nanotubes meaning that conductance is ballistic in nature. Conductance measurements of multi-wall carbon nanotubes raised a significant controversy due to the observation of unexpected conductance values in apparent disagreement with theoretical predictions.[99] In these experiments, multi-wall carbon nanotubes, when brought into contact with liquid mercury, exhibit not only even, but also odd multiples of the conductance quantum $G_0$. An even bigger surprise was the observation of non-integer quantum conductance values, such as $G \approx 0.5\ G_0$.[99] A theoretical study showed that different characters of incident $\pi^*$- and $\pi$-band electrons may be responsible for reducing the conductance from 2 $G_0$ to 1 $G_0$.[100] Another theoretical study explained through the quantum conductance calculations that the quantum conductance reduction to 1 $G_0$ and further to 0.5 $G_0$ is due to the inter-wall interactions that not only block some of the quantum conductance channels, but also redistribute the current nonuniformly over individual tubes across the structure.[101]

There are several computational or modeling studies on ballistic CNT FETs or related molecular transistors. The characteristics of CNT FETs would be quite different from conventional transistors.[102,103] Quantum transport calculations showed that CNT transistors can operate as ballistic FETs with excellent characteristics even when scaled to 10 nm dimensions. It was also shown that an electrostatically defined quantum dot causes resonant tunnelling due to channel inversion at larger gate voltages resulting in a gated resonant-tunnelling device, with negative differential resistance at a tunable threshold.[102]

The gate voltage dependence of the device conductance at low source–drain voltage is examined as follows. For a given gate voltage, the zero-bias conductance is obtained from[104]

$$G = \frac{4e^2}{h}\int P(E)\left[-\frac{\partial f(E)}{\partial E}\right]\mathrm{d}E$$

where $e$ and $h$ are the electronic charge and Plank constant, $E$ is the energy relative to the Fermi level, and $f(E)$ is the Fermi–Dirac distribution function. To calculate the electron transmission probability $P(E)$ across the device at energy $E$, leads are modeled with semi-infinite metals, such as Au, Pd, and a CNT is done as an overlap junction attached to metal leads. Within this model, the junction becomes a finite scattering region, and semi-infinite metals become the external leads attached to the scattering region. Within the scattering region, the full self-consistent potential $V(z)$ is used, while the potentials in the leads are taken

 

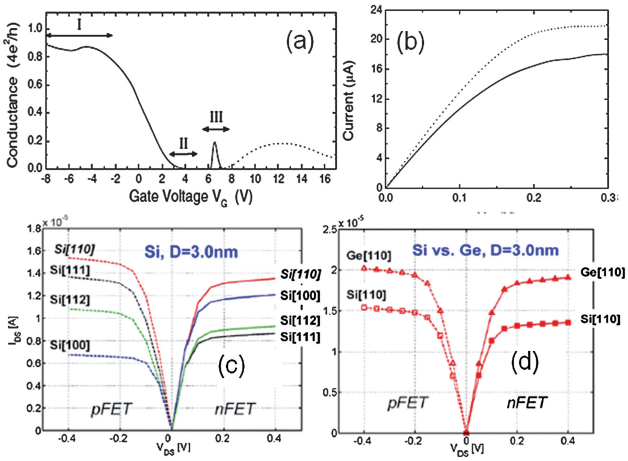


**Fig. 9** (a) Conductance of the nanotube device at low bias. The solid line includes Coulomb-blockade effects, while the dashed line is the result of a standard self-consistent calculation. In the regions I and II, the device exhibits high and zero conductances, respectively, corresponding to the "on" and "off" states of a FET, whereas in III, resonant conductance due to an electrostatically defined quantum dot. (b) Current as a function of drain voltage in the region I ($V_G = -2$ V) described in (a). The solid line is a numerical result for the high transmission model. The dotted line is current in the limit of perfect transmission across the device, for comparison. (c) $I_{DS}$ *vs.* $V_{DS}$ curves for Si NW FETs with four different channel orientations, [100], [110], [111] and [112]. The gate length is $L = 8$ nm, the oxide thickness is 1 nm and the supplied voltage ($V_{DD}$) is 0.4 V. The wire diameter is 3 nm, which offers a good gate control at $L = 8$ nm as well as an acceptable device–device variation. (d) Comparison between Si and Ge NW FETs with the optimum wire orientation, [110]. Images (a) and (b) adapted from Ref. 102, (c) and (d) from Ref. 108.

as a constant equal to the potentials at the boundaries of the scattering region.[105,106]

Fig. 9 (a) and (b) show the $I$-$V_G$ and the $I$-$V_{DS}$ characteristics of such a unique transistor, respectively. In region III, especially, there exists a "resonant" peak, which can be understood in terms of the band diagram of the device. With increasing $V_G$, the bands in the channel are pulled down in energy, and thus near $V_G$ in the region III, conduction band states fall into the band gap resulting in the quantum confinement defining a quantum dot with localized states.[102] Similar to conventional transistors, current through CNT devices saturates with increasing drain voltage as shown in Fig. 9 (b). For a single CNT device, the current is limited mostly by the finite number of available carriers in the leads, whereas for conventional devices as well as for other multiple CNT devices including network devices, the saturation is due to "pinch-off" and/or velocity saturation, which depends on device designs, contact properties, and bias conditions.

Using a semiclassical method, it was shown that the ballistic limit performance of CNT FETs is better than that of ballistic silicon MOSFETs.[107] Moreover, it is reported that their complex band structure may be of importance to determine the subthreshold characteristics of ballistic Si and Ge NW FETs[108] as well as CNT FETs.[109] When its effective mass $m^*$ is large ($m^* > 0.15m_e$), a NW FET operates close to the charge-control limit and the "on" current increases with decreasing $m^*$. Fig. 9 (c) displays this for *n*-doped Si NW FETs (*n*FETs) with four different channel orientations, [100], [110], [111] and [112], where the order of the "on" current magnitudes is exactly the inverse of the order of $m^*$. When $m^*$ is relatively small ($m^* < 0.15m_e$), it operates near the quantum-capacitance-limit and the "on" current is insensitive to $m^*$ but increases with band degeneracy, as shown for Si *p*FETs in Fig. 9 (d).[108] In addition, high-bias transport in single Schottky-barrier contacted semiconducting SWNTs was investigated experimentally to know the electric-field dependence of the carrier velocity by considering four different models: ballistic, current saturation, velocity saturation, and constant mobility.[110] Based on this investigation, the experimental data show the best agreement with the velocity-saturation model with the saturation velocity of $2 \times 10^7$ cm/s.[110]

Although the ballistic characteristic of such FETs is important and interesting for future ballistic device development, it can be observable only in devices with a small channel (smaller than its electronic mean free path) such as single (and short) nanowire devices. In practice, most devices including nanotube network devices described in this review, show little ballistic behaviors.

### 4.2 Understanding sensor operation

Since it was shown that NWs and NTs can be used as FETs, it is natural that they should be used as sensing devices. Indeed they were used to detect various gas molecules.[48,111] Although there are a great deal of issues that should be resolved before such NW- and NT-based sensors replace conventional sensors, they have a variety of advantages over conventional gas, chemical or biological sensors due to larger surface areas resulting in higher sensitivity, smaller size, and lower power consumption, just to name a few. In tandem with experimental tests, there have been various modeling studies in order to understand fundamental sensing mechanisms, which helps experimental research develop further.

NT- and NW-based sensors have been used with a variety of purposes and operated in different ways, such as gas, chemical, biological, strain, stress, pressure, mass, flow, thermal, and optical sensors. Among these, most sensors have been developed based on the modulation of their electronic properties in the presence of target objects (gas, chemical, biological molecules, *etc.*), since the adsorbates on their large surface can easily alter their "surface" electronic states and thus their electronic properties. For such sensing devices, several sensing mechanisms were proposed. One of which suggests that the change in the work function of metal electrodes due to adsorption of external agents, whereas another proposed that charge transfer between external agents and NW FETs would change their electronic characteristics. It was naturally assumed that such modulation was originated by doping due to the charge transfer between adsorbates and NWs. For example, *p*-type CNT FETs were used to detect $NO_2$ and $NH_3$, in the presence of which the conductance increases and decreases, respectively.[48]

A number of experimental results have been successfully explained by this doping mechanism.[48,111-115] There were some other cases that do not fit into the doping explanation.[116] Instead such cases were explained by the change in the work function of metal electrodes due to the adsorption of the external agents resulting in the change in Schottky barrier at the interface. Both explanations can be applied to the change in the electronic properties, but they can be experimentally verified. In the latter

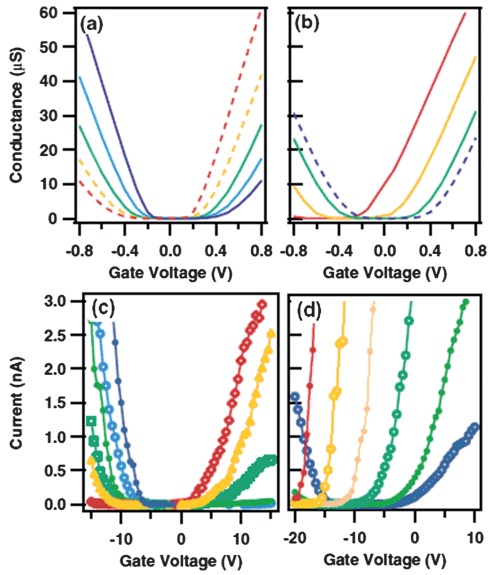


**Fig. 10** (a–b) Calculated conductance *vs.* gate voltage at room temperature, varying (a) the work function of the metal electrode, and (b) doping of the NT. In (a) the work function of the metal electrode is changed by −0.2 eV (red dashed), −0.1 eV (orange dashed), 0 eV (green), +0.1 eV (light blue), and +0.2 eV (blue), from left to right, respectively. In (b) the doping atomic fraction is *n*-type $10^{-3}$ (red), $5 \times 10^{-4}$ (orange), and $10^{-4}$ (green), and *p*-type $10^{-4}$ (blue dashed), from left to right, respectively. (c–d) The experimentally measured effect of (c) oxygen adsorption and (d) potassium doping on NT-FETs. In (c) the annealed (*n*-type) FET has been exposed to oxygen for 2 min at $P = 0$ Torr (red), $P = 10^{-4}$ Torr (orange), $P = 5 \times 10^{-4}$ Torr (light green), $P = 5 \times 10^{-3}$ Torr (dark green), $P = 10^{-1}$ Torr (light blue), and in ambient (blue), from left to right respectively. In (d) the curves from right to left (blue, dark and light green, light and dark orange, red) correspond to increasing deposited amounts of potassium. Images adapted from Ref. 117.

case, the gate-dependent conductance should be tilted since the effect of different concentrations of adsorbates is the change of Schottky barrier. In the former case, the concentration changes do not alter Schottky barrier, but just change the amount of charge transfer, or doping quantity, resulting in the shift of the gate-dependent conductance.[117]

Fig. 10 shows a series of the conductance *vs.* gate voltage of a CNT FET device. Fig. 10 (a) displays varying work functions of the metal electrode, which will change the Schottky barrier at the interface. Fig. 10 (b) is the for varying charge transfer to the CNT, which do not alter the Schottky barrier.[117] As seen in the Fig. 10, the $G$-$V_G$ characteristics show different behaviors for two cases. The work function difference tilts the conductance by lowering for one sign of gate voltage and increasing for the opposite sign. It is also observed that the range of gate voltage remains almost unchanged (Fig. 10 (a)). For doping, in contrast, the conductance shift—to negative gate voltages for *n*-type doping, and to positive gate voltages for *p*-type doping. At a sufficiently high level of doping, a finite conductance is observed even at zero gate voltage (Fig. 10 (b)). These characteristics of calculated conductance are in very good agreement with the experimental measurements shown in Fig. 10 (c) and 10 (d).[116,117]

### 4.3 Anomalous behaviors of network-based transistors

For network-based transistors, we will focus only on CNT networks, which are mixtures of both metallic and semiconducting NTs. In this subsection, we describe the electronic and transport properties of such hybrid nanodevices based on mixed chirality nanotube networks. There have been several modeling and experimental studies on CNT/NW "random" network thin film devices made of random percolating nanotubes or NWs.[118–123] In some studies, limiting cases of ballistic and diffusive regimes were also considered. The former case is hardly observable in real CNT/NW network devices unless the length of CNTs/NWs is longer than the very short channel dimension, which is smaller than the electron mean free path.[118]

We have developed a methodology for modeling electrical properties of nanotube composite thin films, and optimizing the production specifications for yielding the optimal performance while minimizing the number of defective components. Our computational approach is to model the device as a random dispersion of nanotubes. The dispersion can be modeled with fractal diffusion taking into account the lensing effect of the substrate template which imposes alignment of the nanotubes at the channel edges. The dispersion is also represented as a grid of resistors and nodes. Using Kirchhoff's laws with measured and modeled nanotube conductance and nanotube junction conductance, the electronic properties of individual model channels can be estimated. A Monte Carlo approach to statistically characterizing outcomes shows the optimal channel dimensions and nanotube density for resulting in the most semiconducting devices; and models ensemble statistics of the electrical properties of these thin films.

The main difference of our modeling from other modeling studies is based on textured channels, within which CNTs are only deposited implying that CNTs placed at the boundaries of the channel tend to align along the boundary line.[124] Such unique alignment exhibits unusual electrical characteristics in conductivity and mobility,[124] which are not shown in completely random network devices.[125]

Fig. 11 (a) shows a bird's eye view of a mixed chirality network. We can regard it as a system of percolating sticks. Here the red sticks represent metallic nanotubes and the blue sticks represent semiconducting nanotubes. The overlay shows possible subregions that would result from such dispersion on a template. We know from fractal or percolation theories that an infinitely large network of sticks will percolate at a threshold density of $\rho_{Th}$

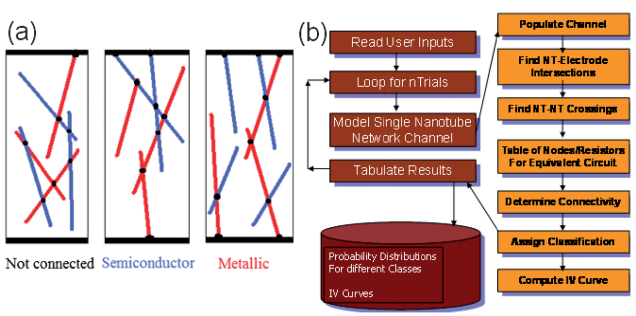


**Fig. 11** (a) Classification of the different chirality of assembled SWNTs in channels. (b) Central algorithm of the model.

$= 4.26^2/\pi L_S^2$ or higher. This value is about 0.64 nanotubes in 1 μm$^2$ for a random dispersion of 3 μm nanotubes. Channels are not infinite in extent, and local regions have three possible connectivity classes as shown in Fig. 11 (a). The first possibility is that connectivity is broken, so that the device lacks a conducting path from electrode to electrode. If all the tubes are semiconducting, high densities would solve this problem. But with mixed chirality, a high density in which the fraction of metallic tubes will result in a device with metallic properties. For the infinite extent channel, when the metallic fraction of tubes is 0.64 NTs/μm$^2$, then the device will be metallic. The second possible outcome is a channel that has a conducting path from electrode to electrode that consists exclusively of metallic tubes. The broken connectivity and the metallic connectivity are undesired outcomes. What industry seeks are techniques for creating semiconducting channels of nanotube networks. The third possible outcome is a channel with at least one semiconducting nanotube along each path of nanotubes connecting the two electrodes. Thus there are three possible classes of devices: not connected, metallic, and semiconducting. Our model can be used to predict the likelihood of each class for a given set of processing parameters.

The inputs to the model are the channel dimensions, fraction of metallic nanotubes, and nanotube density. These are the parameters used to describe a single channel or a single device. The number of trials for the Monte Carlo statistics is also an input and specifies the number of such devices that will be modelled in the simulation. As the model runs it accesses a database of nanotube properties. The model outputs the probability distribution functions for each class. A bias voltage can be specified to model $I$-$V_g$ curves for individual channels.

The program is modular and the database is flexible and extensible. Currently, there are nominal properties for nanotube conductivity operating at room temperatures, in ambient environment, and dispersed on a generic substrate. The program is designed to allow that database to grow and include nanotube properties including alternative algorithms for the dispersion statistics (the position and orientation in the channel) that simulate bundling or other dynamics; and nanotube properties that are environmentally active to address questions of using the thin film as a sensor and modelling that sensor performance or determining when a device might fail; and compare the performance of different chirality mixtures on different substrates.

The central algorithm is shown in Fig. 11 (b). First a channel is modelled by populating it with nanotubes. Internally, the orientation and classification (defining properties) of each nanotube is maintained in a list. Next the locations where nanotubes contact the electrodes and the nanotube junctions in the channel are found. These locations are used to segment the nanotubes into resistors and nodes. This equivalent circuit is analyzed to determine path connectivity and assign a classification: broken, metallic, or semiconducting, to the device channel. The electronic properties are determined by solving the equivalent circuit using WinSpice. Performing this sequence many times to acquire statistics for probability distribution functions of each class as a function of density or other manufacturing variable.

The probability distributions as functions of nanotube density are shown in Fig. 12. The blue line represents the percentage of semiconducting nanotube networks at each density.

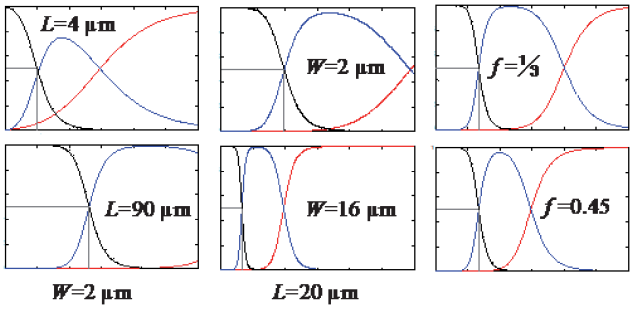


**Fig. 12** Probability distributions as functions of nanotube density with selected manufacturing parameters. The black lines represent "not connected" devices; the blue lines the probability of semiconducting devices at given density, whereas the red ones do for metallic devices.

Manufacturers want a high probability of semiconducting nanotubes, and processing parameters that are not too sensitive to variation. For example, the statistics will ideally not change significantly as the width or length or density changes. Optimally, the high turnout of semiconducting networks will occur for a wide range of densities, not within a narrow peak.[124]

The probability distribution of unconnected networks resembles the Fermi–Dirac distribution function starting with 100% not connecting, having a nearly linear slope near the 50% not connecting point, and ending with 100% connecting. In percolation theory, the percolation threshold characterizes the criteria at which a system will percolate. But this applies generally to systems that are infinite in extent. It is inconvenient to use a percolation threshold to characterize systems of percolating sticks that are directional and finite in extent. A more convenient metric for characterizing connectivity is the reference point at which 50% of the channels percolate. When the channel width is held constant the $\rho_0$ point occurs at higher densities, as channel length is increased.

When the channel length is held constant, the $\rho_0$ point occurs at lower density as width increases. This result is counter intuitive at first glance, when considering percolation as a function of area. But the channel connectivity imposes a directional connectivity. Consider two channels side by side. The probability for both being unconnected follows the product rule, thus 75% will have at least one of the two channels connecting at the single channel $\rho_0$ density point. Thus doubling the channel width substantially increases the number of connecting devices.

The final set in Fig. 12 illustrates the sensitivity to small changes in chirality mix. Even a small change in the fraction of metallic content can result in significant more or less metallic devices.

Our database currently focuses on four resistances for modelling the equivalent circuit. First, measurements of metallic SWNT are length dependent and about 4 kΩ/μm.[126] The conductivity of the semiconducting nanotubes is reported to be length dependent and dependent on the gate voltage.[126–129] Nanotubes have been found to have conductances that vary inversely as length and proportional to applied voltage: [126]

$$G = \mu C_g(V_G - V_{G0})/L$$

where $C_g$ is the capacitance per unit length of the tube, $V_{g0}$ is the threshold voltage, $\mu$ is the mobility, and $L$ is the tube length. Here

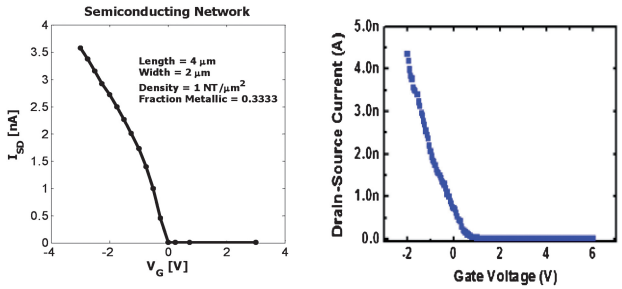


**Fig. 13** $I$-$V_g$ characteristic calculated (left) and experimentally measured one (right).

an array of values is generated to create an $I$-$V$ curve, though the factor of capacitance and mobility can vary significantly. Nanotube mobilities have been measured from 1,000–10,000 $cm^2$/Vs for CVD tubes, and recently a value as high as 200,000 $cm^2$/Vs has been reported for graphene.[129] The electrical measurements were done on various junctions of crossed nanotubes and modelled computationally.[130,131] We used a nominal value of 40 kΩ but these are highly sensitive to pressure so that the network might be useful as an electromechanical sensor. Finally we set the nanotube electrode contacts to 50 kΩ.

The shape of the resulting $I$-$V$ curves resemble those found experimentally. Fig. 13 shows some representative results. We find similar orders of magnitude difference for semiconducting and metallic networks, but the capacitance/mobility factor can change the outcome by orders of magnitude.

We have shown that nanotube networks exhibit excellent semiconducting properties; and it is possible to produce hybrid nanodevices from mixed chirality nanotubes. We have developed a model for estimating the probability of successful and defective semiconductors resulting from a set of manufacturing parameters. For example, over 90% of devices with $40 \times 2$ $\mu m^2$ channel dimension, of 1/3 metallic content, and $\rho = 4$ NTs/$\mu m^2$ will have semiconducting properties.

## 5.0 Conclusions

In summary, NW/CNT-based devices have been a promising new component for LoC applications because they can add various new capabilities to LoC systems such as ultra-sensitive and miniaturized sensors. However, a lack of mass-production methods has been one of the major hurdles holding back the practical applications of such devices. We reviewed several promising strategies to position massive arrays of NWs and CNTs for practical LoC applications. We also discussed NW and CNT based biosensors for practical LoC applications. Futhermore, theoretical understanding of these devices and charateristics of NW/CNT network based FETs were also presented. Considering recent rapid progress of NW/CNT-based devices and their fabrication methods, we believe that it can play a significant role in the future LoC systems such as sensors and other functional devices.

## Acknowledgements

SH acknowledges the support from the Seoul R&DB program (GR070045) and the System 2010 program of the MKE, and the partial support from the Next Generation New Technology Development Program. YKK acknowledges the support in part from UML NCOE, NSF NSEC-CHN (NSF-0425806) and NSF (CMMI-0708541). JOL acknowledges support from the Ministry of Environment as "The Eco-technopia 21 project."

## References

1 S. Iijima, *Nature*, 1991, **354**, 56.
2 Y. Zhang, A. Chang, J. Cao, Q. Wang, W. Kim, Y. Li, N. Morris, E. Yenilmez, J. Kong and H. Dai, *Appl. Phys. Lett.*, 2001, **79**, 3155.
3 S. J. Kang, C. Kocabas, T. Ozel, M. Shim, N. Pimparkar, M. A. Alam, S. V. Rotkin and J. A. Rogers, *Nat. Nanotechnol.*, 2007, **2**, 230.
4 J. H. He, J. H. Hsu, C. W. Wang, H. N. Lin, L. J. Chen and Z. L. Wang, *J. Phys. Chem. B*, 2006, **110**, 50.
5 T. Martensson, M. Borgstrom, W. Seifert, B. J. Ohlsson and L. Samuelson, *Nanotechnology*, 2003, **14**, 1255.
6 K. Kempa, B. Kimball, J. Rybczynski, Z. P. Huang, P. F. Wu, D. Steeves, M. Sennett, M. Giersig, D. V. G. L. N. Rao, D. L. Carnahan, D. Z. Wang, J. Y. Lao, W. Z. Li and Z. F. Ren, *Nano Lett.*, 2003, **3**, 13.
7 T. Martensson, P. Carlberg, M. Borgstrom, L. Montelius, W. Seifert and L. Samuelson, *Nano Lett.*, 2004, **4**, 699.
8 Z. H. Wu, X. Y. Mei, D. Kim, M. Blumin and H. E. Ruda, *Appl. Phys. Lett.*, 2002, **81**, 5177.
9 Y. Xia and G. M. Whitesides, *J. Am. Chem. Soc.*, 1995, **117**, 3274.
10 J. R. Heath and F. K. Legoues, *Chem. Phys. Lett.*, 1993, **208**, 263.
11 T. J. Trentler, K. M. Hickman, S. C. Geol, A. M. Viano, P. C. Gibbons and W. E. Buhro, *Science*, 1995, **270**, 1791.
12 L. Ouyang, K. N. Maher, C. L. Yu, J. McCarty and H. Park, *J. Am. Chem. Soc.*, 2007, **129**, 133.
13 X. Peng, L. Manna, W. Yang, J. Wickham, E. Scher, A. Kadavanich and A. P. Alivisatos, *Nature*, 2000, **404**, 59.
14 L. Manna, E. C. Scher and A. P. Alivisatos, *J. Am. Chem. Soc.*, 2000, **122**, 12700.
15 Y. Sun, B. Gates, B. Mayers and Y. Xia, *Nano Lett.*, 2002, **2**, 165.
16 L. Vayssieres, *Adv. Mater.*, 2003, **15**, 464.
17 J. Muster, G. T. Kim, V. Krstic, J. G. Park, Y. W. Park, S. Roth and M. Burghard, *Adv. Mater.*, 2000, **12**, 420.
18 P. A. Smith, C. D. Nordquist, T. N. Jackson, T. S. Mayer, B. R. Martin, J. Mbindyo and T. E. Mallouk, *Appl. Phys. Lett.*, 2000, **77**, 1399.
19 R. Krupke, F. Hennrich, H. v. Löhneysen and M. M. Kappes, *Science*, 2003, **301**, 344.
20 X. Duan, Y. Huang, Y. Cui, J. Wang and C. M. Lieber, *Nature*, 2001, **409**, 66.
21 T. J. Morrow, M. Li, J. Kim, T. S. Mayer and C. D. Keating, *Science*, 2009, **323**, 352.
22 Y. Huang, X. Duan, Q. Wei and C. M. Lieber, *Science*, 2001, **291**, 630.
23 D. Whang, S. Jin and C. M. Lieber, *Nano Lett.*, 2003, **3**, 951.
24 A. Tao, F. Kim, C. Hess, J. Goldberger, R. R. He, Y. G. Sun, Y. N. Xia and P. D. Yang, *Nano Lett.*, 2003, **3**, 1229.
25 D. Whang, S. Jin, Y. Wu and C. M. Lieber, *Nano Lett.*, 2003, **3**, 1255.
26 M. Tanase, D. M. Silevitch, A. Hultgren, L. A. Bauer, P. C. Searson, G. J. Meyer and D. H. Reich, *J. Appl. Phys.*, 2002, **91**, 8549.
27 C. M. Hangarter, Y. Rheem, B. Yoo, E. H. Yang and N. V. Myung, *Nanotechnology*, 2007, **18**, 205305.
28 J. Liu, M. J. Casavant, M. Cox, D. A. Walters, P. Boul, W. Lu, A. J. Rimberg, K. A. Smith, D. T. Colbert and R. E. Smalley, *Chem. Phys. Lett.*, 1999, **303**, 125.
29 S. G. Rao, L. Huang, W. Setyawan and S. Hong, *Nature*, 2003, **425**, 36.
30 M. Lee, J. Im, B. Y. Lee, S. Myung, J. Kang, L. Huang, Y.-K. Kwon and S. Hong, *Nat. Nanotechnol.*, 2006, **1**, 66.
31 S. Myung, M. Lee, G. T. Kim, J. S. Ha and S. Hong, *Adv. Mater.*, 2005, **17**, 2361.
32 B. Y. Lee, Y. W. Kim, D. J. Lee and S. Hong, *Biochip J.*, 2007, **1**, 76.
33 R. D. Piner, J. Zhu, F. Xu, S. Hong and C. A. Mirkin, *Science*, 1999, **283**, 661.
34 P. Manandhar, J. Jang, G. C. Schatz, M. A. Ratner and S. Hong, *Phys. Rev. Lett.*, 2003, **90**, 115505.

 

35 A. K. Salem, J. Chao, K. W. Leong and P. C. Searson, *Adv. Mater.*, 2004, **16**, 268.
36 M. Chen and P. C. Searson, *Adv. Mater.*, 2005, **17**, 2765.
37 J. K. N. Mbindyo, B. D. Reiss, B. R. Martin, C. D. Keating, M. J. Natan and T. E. Mallouk, *Adv. Mater.*, 2001, **13**, 249.
38 K. Heo, E. Cho, J.-E. Yang, M.-H. Kim, M. Lee, B. Y. Lee, S. G. Kwon, M.-S. Lee, M.-H. Jo, H.-J. Choi, T. Hyeon and S. Hong, *Nano Lett.*, 2008, **12**, 4523.
39 E. Menard, K. J. Lee, D. Y. Khang, R. G. Nuzzo and J. A. Rogers, *Appl. Phys. Lett.*, 2004, **84**, 5398.
40 Y. G. Sun and J. A. Rogers, *Nano Lett.*, 2004, **4**, 1953.
41 M. A. Meitl, Z. T. Zhu, V. Kumar, K. J. Lee, X. Feng, Y. Y. Huang, I. Adesida, R. G. Nuzzo and J. A. Rogers, *Nat. Mater.*, 2006, **5**, 33.
42 Q. Cao, H.-s. Kim, N. Pimparkar, J. P. Kulkarni, C. Wang, M. Shim, K. Roy, M. A. Alam and J. A. Rogers, *Nature*, 2008, **454**, 495.
43 Y.-K. Kim, S. J. Park, J. P. Koo, D.-J. Oh, G. T. Kim, S. Hong and J. S. Ha, *Nanotechnology*, 2006, **17**, 1375.
44 Z. Fan, J. C. Ho, Z. A. Jacobson, R. Yerushalmi, R. L. Alley, H. Razavi and A. Javey, *Nano Lett.*, 2008, **8**, 20.
45 A. Javey, S. Nam, R. S. Friedman, H. Yan and C. M. Lieber, *Nano Lett.*, 2007, **7**, 773.
46 A. Stikeman, *Technology review*, May 2002, p61.
47 Y. Cui, Q. Wei, H. Park and C. M. Lieber, *Science*, 2001, **293**, 1289.
48 J. Kong, N. R. Franklin, C. Zhou, M. G. Chaplin, S. Peng, K. Cho and H. Dai, *Science*, 2000, **287**, 622.
49 C. Li, M. Curreli, H. Lin, B. Lei, F. Ishikawa, R. Datar, R. Cote, M. Thomson and C. Zhou, *J. Am. Chem. Soc.*, 2005, **127**, 12484.
50 J. S. Kim, W. I. Park, C.-H. Lee and G.-C. Yi, *J. Kor. Phys. Soc.*, 2006, **49**, 1635.
51 F. Patolsky, G. Zheng, O. Hayden, M. Lakadamyali, X. Zhuang and C. M. Lieber, *Proc. Natl. Acad. Sci. USA*, 2004, **101**, 14017.
52 G. Zheng, F. Patolsky, Y. Cui, W. U. Wang and C. M. Lieber, *Nat. Biotechnol.*, 2005, **23**, 1294.
53 E. Stern, J. F. Klemic, D. A. Routenberg, P. N. Wyrembak, D. B. Turner-Evans, A. D. Hamilton, D. A. La Van, T. M. Fahmy and M. A. Reed, *Nature*, 2007, **445**, 519.
54 E. Menard, K. J. Lee, D.-Y. Khang, R. G. Nuzzo and J. A. Rogers, *Appl. Phys. Lett.*, 2004, **84**, 5398.
55 J. Hahm and C. M. Lieber, *Nano Lett.*, 2004, **4**, 51.
56 W. U. Wang, C. Chen, K. Lin, Y. Fang and C. M. Lieber, *Proc. Natl. Acad. Sci. USA*, 2005, **102**, 3208.
57 S. J. Tans, A. R. M. Verschueren and C. Dekker, *Nature*, 1998, **393**, 49.
58 A. Javey, J. Guo, Q. Wang, M. Lundstrom and H. Dai, *Nature*, 2003, **424**, 654.
59 www.nano.com.
60 H.-M. So, B.-K. Kim, D.-W. Park, B. S. Kim, J.-J. Kim, K. Kong, H. Chang and J.-O. Lee, *J. Am. Chem. Soc.*, 2007, **129**, 4866.
61 P. G. Collins, M. S. Arnold and P. Avouris, *Science*, 2001, **292**, 706.
62 M. S. Arnold, A. A. Green, J. F. Hulvat, S. I. Stupp and M. C. Hersam, *Nat. Nanotechnol.*, 2006, **1**, 60.
63 M. C. Hersam, *Nat. Nanotechnol.*, 2008, **3**, 387.
64 S. Wang, E. S. Humphreys, S. Y. Chung, D. F. Delduco, S. R. Lustig, H. Wang, K. N. Parker, N. W. Rizzo, S. Subramoney, Y. M. Chiang and A. Jagota, *Nat. Mater.*, 2003, **2**, 196.
65 X. Yu, S. N. Kim, F. Papadimitrakopoulos and J. F. Rusling, *Mol. BioSyst.*, 2005, **1**, 70.
66 J. V. Veetil and K. Ye, *Biotechnology Progress*, 2007, **23**, 517.
67 R. J. Chen, S. Bangsaruntip, K. A. Drouvalakis, N. W. Kam, M. Shim, Y. Li, W. Kim, P. J. Utz and H. Dai, *Proc. Natl. Acad. Sci. USA*, 2003, **100**, 4984.
68 D. W. Park, Y. H. Kim, B. S. Kim, H.-M. So, K. Won, J.-O. Lee, K. Kong and H. Chang, *J. Nanosci. Nanotechnol.*, 2006, **6**, 3499.
69 R. J. Chen, H. C. Choi, S. Bangsaruntip, E. Yenilmez, X. Tang, Q. Wang, Y. L. Chang and H. Dai, *J. Am. Chem. Soc.*, 2004, **126**, 1563.
70 I. Heller, A. M. Janssens, J. Mannik, E. D. Minot, S. G. Lemay and C. Dekker, *Nano Lett.*, 2008, **8**, 591.
71 X. Tang, S. Bangsaruntip, N. Nakayama, E. Yenilmez, Y. I. Chang and Q. Wang, *Nano Lett.*, 2006, **6**, 1632.
72 E. L. Gui, L.-J. Li, K. Zhang, Y. Xu, X. Dong, X. Ho, P. S. Lee, J. Kasim, Z. X. Shen, J. A. Rogers and S. G. Mhaisalkar, *J. Am. Chem. Soc.*, 2007, **129**, 14427.
73 H. R. Byon and H. C. Choi, *J. Am. Chem. Soc.*, 2006, **128**, 2188.
74 J.-O. Lee, H.-M. So, E.-K. Jeon, H. Chang, K. Won and Y. H. Kim, *Anal. Bioanal. Chem.*, 2008, **390**, 1023.
75 H.-M. So, K. Won, Y. H. Kim, B.-K. Kim, B. H. Ryu, P. S. Na, H. Kim and J.-O. Lee, *J. Am. Chem. Soc.*, 2005, **127**, 11906.
76 K. Maehashi, T. Katsura, K. Kerman, Y. Takamura, K. Matsumoto and E. Tamiya, *Anal. Chem.*, 2007, **79**, 782.
77 J. P. Kim, B. Y. Lee, S. Hong and S. J. Sim, *Anal. Biochem.*, 2008, **381**, 193.
78 T. M. Squires, R. J. Messinger and S. R. Manalis, *Nat. Biotechnol.*, 2008, **26**, 427.
79 H.-M. So, D.-W. Park, E.-K. Jeon, Y.-H. Kim, B. S. Kim, C.-K. Lee, S. Y. Choi, S. C. Kim, H. Chang and J.-O. Lee, *Small*, 2008, **4**, 197.
80 G. Schreiber, *Curr. Opin. Struct. Biol.*, 2002, **12**, 41.
81 S. K. Yoon, G. W. Fichtl and P. J. A. Kenis, *Lab Chip*, 2006, **6**, 1516.
82 R. A. Vijayendran, K. M. Motsegood, D. J. Beebe and D. E. Leckband, *Langmuir*, 2003, **19**, 1824.
83 C.-H. Hsu, D. Di Carlo, C. Chen, D. Irimia and M. Toner, *Lab Chip*, 2008, **8**, 2128.
84 G. E. Moore, *Electronics*, 1965, (8), 38.
85 J. V. der Spiegel, in *Introduction to Nanoscale Science and Technology*, ed. M. Di Ventra, S. Evoy and J. R. Heflin, Jr., Springer, New York, 2004, p. 217.
86 M. Bockrath, D. H. Cobden, P. L. McEuen, N. G. Chopra, A. Zettl, A. Thess and R. E. Smalley, *Science*, 1997, **275**, 1922.
87 R. Martel, T. Schmidt, H. R. Shea, T. Hertel and Ph. Avouris, *Appl. Phys. Lett.*, 1998, **73**, 2447.
88 S.-W. Chung, J.-Y. Yu and J. R. Heath, *Appl. Phys. Lett.*, 2000, **76**, 2068.
89 Y. Huang, X. Duan, Y. Cui and C. M. Lieber, *Nano Lett.*, 2002, **2**, 101.
90 Z. Zhong, F. Qian, D. Wang and C. M. Lieber, *Nano Lett.*, 2003, **3**, 343.
91 D. Zhang, C. Li, S. Han, X. Liu, T. Tang, W. Jin and C. Zhou, *Appl. Phys. Lett.*, 2003, **82**, 112.
92 M. S. Arnold, P. Avouris, Z. W. Pan and Z. L. Wang, *J. Phys. Chem. B*, 2003, **107**, 659.
93 L. Chico, L. X. Benedict, S. G. Louie and M. L. Cohen, *Phys. Rev. B*, 1996, **54**, 2600.
94 W. Tian and S. Datta, *Phys. Rev. B*, 1994, **49**, 5097.
95 M. F. Lin and K. W.-K. Shung, *Phys. Rev. B*, 1995, **51**, 7592.
96 R. Landauer, *Phil. Mag.*, 1970, **21**, 863.
97 S. J. Tans, M. H. Devoret, H. Dai, A. Thess, R. E. Smalley, L. J. Geerligs and C. Dekker, *Nature*, 1997, **386**, 474.
98 M. S. Purewal, B. H. Hong, A. Ravi, B. Chandra, J. Hone and P. Kim, *Phys. Rev. Lett.*, 2007, **98**, 186808.
99 S. Frank, P. Poncharal, Z. L. Wang and W. A. de Heer, *Science*, 1998, **280**, 1744.
100 H. J. Choi, J. Ihm, Y.-G. Yoon and S. G. Louie, *Phys. Rev. B*, 1999, **60**, R14009.
101 S. Sanvito, Y.-K. Kwon, D. Tománek and C. J. Lambert, *Phys. Rev. Lett.*, 2000, **84**, 1974.
102 F. Léonard and J. Tersoff, *Phys. Rev. Lett.*, 2002, **88**, 258302.
103 A. D. Carlo, M. Gheorghe, P. Lugli, M. Sternberg, G. Seifert and T. Frauenhein, *Physica B*, 2002, **314**, 86.
104 S. Datta, in *Electronic Transport in Mesoscopic Systems*, ed. H. Ahmed, M. Pepper and A. Broers, Cambridge University Press, Cambridge, 1995.
105 M. Büttiker, Y. Imry, R. Landauer and S. Pinhas, *Phys. Rev. B*, 1985, **31**, 6207.
106 S. Sanvito, C. J. Lambert, J. H. Jefferson and A. M. Bratkovsky, *Phys. Rev. B*, 1999, **59**, 11936.
107 J. Guo, M. Lundstrom and S. Datta, *Appl. Phys. Lett.*, 2002, **80**, 3192.
108 J. Wang, A. Rahman, G. Klimeck and M. Lundstrom, *IEEE Int. Electron Devices Meetings*, 2005, 530.
109 T.-S. Xia, L. F. Register and S. K. Banerjee, *J. Appl. Phys.*, 2004, **95**, 1597.
110 Y.-F. Chen and M. S. Fuhrer, *Phys. Rev. Lett.*, 2005, **95**, 236803.
111 P. G. Collins, K. Bradley, M. Ishigami and A. Zettl, *Science*, 2000, **287**, 1801.
112 S. Peng, K. Cho, P. Qi and H. Dai, *Chem. Phys. Lett.*, 2004, **387**, 271.
113 S. Peng and K. Cho, *Nanotechnology*, 2000, **11**, 57.

114 H. Chang, J. D. Lee, S. M. Lee and Y. H. Lee, *Appl. Phys. Lett.*, 2001, **79**, 3863.
115 J. Zhao, A. Buldum, J. Han and J. P. Lu, *Nanotechnology*, 2002, **13**, 195.
116 V. Derycke, R. Martel, J. Appenzeller and Ph. Avouris, *Appl. Phys. Lett.*, 2002, **80**, 2773.
117 S. Heinze, J. Tersoff, R. Martel, V. Derycke, J. Appenzeller and P. Avouris, *Phys. Rev. Lett.*, 2002, **89**, 106801.
118 S. Kumar, J. Y. Murthy and M. A. Alam, *Phys. Rev. Lett.*, 2005, **95**, 066802.
119 N. Pimparkar, Q. Cao, J. A. Rogers and M. A. Alam, *Nano Res.*, 2009, **2**, 167.
120 Q. Cao, H.-S. Kim, N. Pimparkar, J. P. Kulkarni, C. Wang, M. Shim, K. Roy, M. A. Alam and J. A. Rogers, *Nature*, 2008, **454**, 495.
121 N. Pimparkar, C. Kocabas, S. J. Kang, J. Rogers and M. A. Alam, *IEEE Electron Dev. Lett.*, 2007, **28**, 593.
122 N. Pimparkar, Q. Cao, S. Kumar, J. Y. Murthy, J. Rogers and M. A. Alam, *IEEE Electron Dev. Lett.*, 2007, **28**, 157.
123 C. Kocabas, N. Pimparkar, O. Yesilyurt, S. J. Kang, M. A. Alam and J. A. Rogers, *Nano Lett.*, 2007, **7**, 1195.
124 M. Lee, M. Noah, J. Park, M.-J. Seong, Y.-K. Kwon and S. Hong, *Small*, 2009, in press.
125 A. Behnam, L. Noriega, Y. Choi, Z. Wu, A. G. Rinzler and A. Ural, *Appl. Phys. Lett.*, 2006, **89**, 093107.
126 P. L. McEuen and J.-Y. Park, *MRS Bull.*, 2004, **29**, 272.
127 P. J. Burke, *Proc. IEEE-NANO*, 2002, 393.
128 S. Llani, L. A. K. Donev, M. Kindermann and P. L. McEuen, *Nat. Phys.*, 2006, **2**, 687.
129 K. I. Bolotin, K. J. Sikes, Z. Jiang, M. Klima, G. Gudenberg, J. Hone, P. Kim and H. L. Stormer, *Solid State Commun.*, 2008, **146**, 351.
130 M. S. Fuhrer, J. Nygard, L. Shih, M. Forero, Y.-G. Yoon, M. S. C. Mazzoni, H. J. Choi, J. Ihm, S. G. Louie, A. Zettl and P. L. McEuen, *Science*, 2000, **288**, 494.
131 Y.-G. Yoon, M. S. C. Mazzoni, H. J. Choi, J. Ihm and S. G. Louie, *Phys. Rev. Lett.*, 2001, **86**, 688.

 